Evaluation of flow characteristics that give higher mixing performance in the 3-D T-mixer versus the typical T-mixer

Cesar Augusto Cortes-Quiroz[a,b*], Alireza Azarbadegan[b], Mehrdad Zangeneh[b]

[a] Science and Technology Research Institute, University of Hertfordshire, College Lane, Hatfield, Herts, AL10 9AB, UK

[b] Department of Mechanical Engineering, University College London, Torrington Place, London, WC1E 7JE, UK

*Author for correspondence
Email: c.cortes-quiroz@herts.ac.uk *Phone*: +44 (0) 1707284147 *Fax*: +44 (0) 1707281306

Abstract

A 3-D configuration of a T-mixer is evaluated under normal operating conditions of the called convective micromixers. The design has been called 3-D T-mixer in our previous work [1] as it adopts a three-dimensional structure at the T-junction. This design feature has been found that it exerts a strong effect on the flow characteristics in the device downstream in the mixing channel. A numerical study has been carried out in the 3-D T-mixer and the typical T-mixer, being these modelled with equal dimensions of channel lengths and cross sections and operated with the same flow rates. The flow analysis in the 3-D T-mixer reveals the quick formation of vortical flow structures composed of intertwined fluid filaments which increase drastically the fluids interface to enhance mixing. The flow patterns in the mixing channel vary with Reynolds number (Re) in the range of 100 to 500.
This study shows that the 3-D T-mixer provides a significant enhancement of mixing and presents lower pressure loss and similar level of shear stress compared to a typical T-mixer, in the whole range of Re used to characterize the flow. It has a simple channel configuration which is easy to fabricate and effective for mixing of continuous fluid and potentially particles. The 3-D T-mixer is called to be tested and applied for improving the efficiency of systems which have a T-junction in their design and require fast mixing with high throughput.

Keywords: Microfluidics, Convective micromixer, 3-D T-mixer, Continuous mixing, Vortex generation, Vortical flow

1. Introduction

In the recent years, microstructured equipments have found applications in processes such as chemical synthesis [2] where a fast mixing is desirable in high throughput systems, i.e., the volume and the rate of generation of products are both important. The volume rate of the products can be increased by raising the flow rate, i.e., by increasing the Re number of flow of reactant fluids. Because flow rates are directly proportional to the levels of transport pressure, it becomes necessary to increase the cross section of the microchannels and to avoid complex structures or obstacles in the channels that may induce higher resistance to the flow. Therefore, it is important that a design could provide good mixing characteristics with high mass flow rates and tolerable pressure losses.
Often, microdevices consist of several long, straight channels with straight laminar flow where diffusion is the only mechanism that governs mass transfer. The flow pattern and the mixing mechanism change when bent and curved channels are included as geometric features that help to generate secondary flows with velocity components perpendicular to

the main flow direction. These flow characteristics can also be achieved in channels with a rectangular cross-section where vortices are formed at Re numbers larger than 10 [3]. This mixing strategy can be applied on the simple T or Y-shaped micromixer by forming a complex flow structure at the entrance of the mixing channel.

In general, most micromixer designs use a T or Y junction for the initial contact of the fluids to be mixed. The typical T and Y shape designs have been tested numerically and experimentally [4-6] to show good mixing for Re in the order of 200 or higher but being ineffective for lower Re values. Therefore, different modifications in design have been introduced with the aim of increasing the effect of advection in mixing, including obstacles within the channel [7, 8], complex channel arrangement such as two dimensional [9] or three dimensional [10] serpentine design of outlet channel, and wall channel structures such as ridges and grooves [11, 12].

Nevertheless, the above designs present more complexity in their fabrication and integration with other microfluidic components. To have simple designs, a solution is to take advantage of flow structures and instabilities in the initial mixing region of the device. An optimization focused on geometric features and flow conditions can be made to achieve more efficient mixing. Few studies have been made with this approach to design. Gobby et al. [4] evaluated numerically the T-type microfluidic mixer in 2-D to identify the mixing characteristics for gas flow and the effect of fluid speed and some design parameters on the required mixing length. Wong et al. [6] used experiments and numerical simulations in micro T-mixers to determine the effect on mixing of asymmetrical flow conditions at the inlets and the generation of vortices and secondary flows at the junction. Bothe et al. [13] evaluated the mixing characteristics of a T-shaped micromixer for three different flow regimes to conclude that only the so-called engulfment flow with intertwinement of the input streams leads to efficient mixing by rolling up the initial planar contact area. Kockmann et al. [14, 15] presented the design, fabrication and mixing characteristics of different mixer configurations, three variations of the T-mixer and one tangential mixer, which give a high throughput of aqueous solutions with mixing enhanced by vortical structures formed inside the micromixers. Yang et al. [16] proposed a passive micromixer in which mixing is enhanced by a large 3-D flow vortex generated in a chamber where two counterflow fluids are self-driven by surface tension. More recently, Matsunaga and Nichino [17] included a pair of antisymmetric barriers in the inlet channels near the junction zone of the T-mixer, which generate angular momentum in the flow inducing a swirling flow structure to improve fluid mixing for $Re > 20$.

In this paper, a new configuration of the T-shaped micromixer, which has been called the 3-D T-mixer [1], is studied. The motivation has been to define a simple channel structure where secondary flows can be generated to enhance mixing but at lower flow rates and, consequently, with lower pressure losses than in the simple planar T-mixer. The basic design of the new channel configuration was born from the intuitive idea of a geometry that can promote flow circulations at different flow rates and not merely because of the presence of obstacles in the device or a high flow rate in the mixing channel. Recently, Ansari et al. [18] provided a valid experimental test of the concept design originally presented by Cortes-Quiroz et al [1]. Their work was applied on a particular configuration of the 3-D T-mixer with aspect ratio of the mixing channel equal to 0.9, where only measurements of mixing level were used to compare its performance against that of a simple T-mixer. Experiments were restricted to a low range of Re of 10 to 70, in which convective effects of flow in the devices are not much strong. Therefore, a clear rise of mixing in the 3-D T-mixer could only be observed with $Re > 40$, reaching a mixing quality of about 50% with $Re = 70$ in 7 mm channel length, while the simple T-mixer presented an almost constant mixing quality of about 11% at all Reynolds numbers.

In the present study, the original geometry of the 3-D T-mixer (aspect ratio of the mixing channel equal to 2.0) [1] has been used to evaluate numerically the flow structures and mixing performance in the device at different Re values. As not only the mixing level achieved in the designs reflects their performance, other important variables such as pressure drop and shear stress have been also evaluated. These are compared to those in a simple T-shaped micromixer which has the same channel lengths and cross-section dimensions. The results show that the key for mixing enhancement is in the flow characteristics developed in the 3-D T-junction and the mixing channel compared to those in the 2-D T-shaped micromixer.

2. Micromixer design

Fig. 1 shows the generic schematics of the three-dimensional T-shaped micromixer. The basic T-shaped micromixer has been modified to have the two inlet channels at different Z-coordinates. The two inlet channels and the straight mixing channel are connected in a T-junction which is defined by the difference in Z-coordinate of the top wall of the higher inlet channel and the bottom wall of the lower inlet channel. The difference of these coordinates, i.e., the height of the mixing channel, and the width of the mixing channel define the geometry of the T-junction of the micromixer.
In the proposed geometry, the inlet channels have been modelled with square cross section since this shape minimizes the pressure loss for the same volume flow rate. The cross section of the inlet channels and mixing channel are h100 x w100 μm and H200 x W100 μm respectively, i.e., the bottom wall of one of the inlet channels is on the same horizontal plane or Z-coordinate than the top wall of the opposite inlet channel. The aspect ratio of the mixing channel, H/W = 2, is equal to the most commonly value used for the ratio W/H in the 2-D T-mixer (H/W = 0.5). Thereby, this geometry of the 2-D T-mixer has the same cross section area of channels as in the 3-D T-mixer. This allows the comparison of flow and mixing at the same flow rate (Re) in both devices.

<Fig. 1>

3. Numerical analysis

Numerical analyses of flow and mixing in the 3-D T-mixer have been performed using the commercial code CFX 12.0 [19].
Since that a high quality mesh is critical to achieve accurate results, especially for mixing analyses, the mesh generator code GRIDGEN 15.1 [20] was used to make a hexahedral grid in the whole model domain. As complex and rotational flows are expected to happen in the model, in particular at medium and high Reynolds number in the mixing channel, the structured mesh provides the advantage of better control in completely packing the corners with a sufficient number of nodes as compared to unstructured mesh for analyzing the effect of geometry on mixing.
Numerical simulations are not free from numerical diffusion error, which arises from the discretization of the convection terms in the Navier-Stokes equation. In this study, to minimize numerical diffusion in the results, the advection terms have been discretized by using a bounding second order differencing scheme, which is an upwind scheme with a second order correction [21]. While the presence of numerical diffusion in the solutions cannot be completely eliminated, it can be reduced by adopting certain techniques. Hardt and Schönfeld [22] found numerical diffusion can be minimized by selecting the edges of mesh cells parallel to local flow velocity. Although this is a condition difficult to attain everywhere in the central channel where mixing is produced, especially in the T joint where

flow field is complex, a high density of the grid can be used. Fig. 2a shows a view of the structured mesh used in the 3-D T-mixer model. The detail shows the distribution of the mesh over the length of the inlet channels and on the cross section of the mixing channel. In the central part of the mixing channel and in zones adjacent to walls, the density of the mesh is clearly higher with a cells size slightly over 1 μm.
A mesh dependency test was carried out to find the optimal size of cells in the models and to ensure the solution is independent of the mesh size. The mixing index, a mixing level measure which is defined later with Eq. (1), was calculated on several cross sections along the mixing channel with an increasing number of mesh cells. Six structured mesh models with the number of cells ranging from about 3000 to 5100 thousands were tested, as shown in Fig. 2b. From the results of the mesh dependency test, the fourth mesh (4' 315 279 cells) with cells size in the range 1.17 to 4.86 μm was selected as the reference size for all the designs modelled in this study.

<Fig. 2>

The flow is defined as viscous, isothermal, incompressible and laminar. The boundary conditions at the two inlets have been set by the fixed uniform velocity. The velocity values at the inlets are equal and give a laminar flow regime with Reynolds numbers in the range 100-250 in the mixing channel. Along the walls, non-slip boundary condition is assigned for the tangential velocity component whereas the normal component is zero. At the outlet, a zero static relative pressure is set.
Water at 25 ºC and a solution of Fluorescein in water are the fluids used in the study. The physical properties of the solution have been considered the same as the ones of water (density, ρ_{H2O} = 997 kg / m^3; dynamic viscosity, μ_{H2O} = 8.899E-04 kg / m.s). The diffusion coefficient of the fluorescein solution in water is taken as D = 1.5 x 10E-09 m^2/s [23]. The boundary conditions for the species balance are mass fractions equal to 0 at the inlet where pure water is fed and equal to 1 at the inlet where the fluorescein solution is fed. It has been considered that simulations converge when the normalized residual (root mean square error) of the mass fraction reaches the value of 1 x 10E-05.
The two metrics calculated from simulations are the mixing index and the pressure drop in the mixing channel. The mixing index, *Mi,* evaluates the degree of mixing achieved in the mixing channel on the basis of the intensity of segregation introduced by Danckwerts [24] and calculated with Eq. (1):

$$Mi = 1 - \sqrt{\frac{\int_A (c - \bar{c})^2 \, \mathrm{d}A}{A \cdot \bar{c}\,(1 - \bar{c})}} \tag{1}$$

where c is the concentration distribution at a defined cross-section of the mixing channel, $\bar{c}$ is the averaged value of the concentration field on the plane and A is the area of the plane. Mi reaches a value of 0 for a complete segregated system and a value of 1 for the homogeneously mixed case.
The pressure drop in the mixing channel is evaluated by the difference between the area-weighted average of total pressure on the outlet plane and on a cross section plane at the inlet of the mixing channel.

4. Results and discussion

The original design of the 3-D T-shaped micromixer has been labelled Orig2.0H to indicate that the aspect ratio of its mixing channel is equal to 2 (H = 200 μm, W = 100 μm). The T-

shaped micromixer with rectangular cross section of aspect ratio equal to 0.5 (H = 100 μm, W = 200 μm) has been labelled AR0.5. The cross sections of inlet channels and mixing channels have the same area in both designs. Therefore, the inlet velocities in the designs are made equal to compare the mixing achieved in them for different Re numbers.

Previous investigations [5, 13] have shown that different flow regimes are developed in the T-shaped micromixer depending on the Re number in the mixing channel. At low Re number values up to 10, the flow is symmetric straight and laminar. Increasing the Re number to around 100 results in formation of symmetric vortices at the entrance of the mixing channel. At a certain critical Re number, a breakup of the flow symmetry is produced, which enhances mixing of the fluids due to the increment of their contact surface. In this section, the flow regimes formed in the T-shaped micromixer AR0.5 for Re numbers between 100 and 500 are examined and compared to the flow characteristics in the 3-D T-shaped micromixer Orig2.0H.

For Re = 100, Fig. 3a shows a view of the streamlines of both fluids coming into the mixing channel of the T-shaped micromixer AR0.5. The two fluids flow along the channel without sweeping their positions and the contact surface is only formed at the symmetry vertical plane of the channel. Therefore, mixing only occurs because of the slow diffusion process, as one can see in Fig. 3b which shows the mass fraction contours of the solution of fluorescein in water on cross sections at the inlet and outlet sections of the mixing channel.

<Fig. 3>

For the same flow boundary conditions, i.e., same inlet velocities for Re = 100 in the mixing channel, Fig. 4a shows the streamlines viewed from the outlet section and Fig. 4b and c show the components of velocity vectors on cross sections at 0.4 mm and 1.6 mm in the mixing channel of design Orig2.0H. The flow looks almost symmetric with respect to a horizontal plane centred in the mixing channel. The vectors show the formation of a big central vortex and two much smaller vortices, with the latter two rotating in opposite direction to the former. Unlike the flow in design AR0.5, an engulfment flow is achieved with Re = 100 in design Orig2.0H, since that a swapping of fluids occurs between both zones of the mixing channel (top and bottom halves), as shown by the streamlines in Fig. 4a. The mass fraction contours at several cross sections of the mixing channel are shown in. The reduction on magnitude of flow circulation along the channel limits the rotation angle which finishes approximately between 630 and 720 degrees at a distance between 0.4 mm and 0.8 mm in the mixing channel, as can be inferred from the contours in Fig. 4d.

<Fig. 4>

For Re = 250, Fig. 5a shows the streamlines viewed from the outlet section and Fig. 5b and c show the components of velocity vectors on cross sections at 0.4 mm and 1.6 mm in the mixing channel of design AR0.5. Clearly, the symmetry of the flow structure with Re = 100 (see Fig. 3a) breaks up with Re = 250. Fluid from one side is swapped to the opposite side due to a double vortex formed at the T-junction and the inlet of the mixing channel. The small vectors in Fig. 5c indicate that the rotation lowers in magnitude along the channel.

This effect can be seen in Fig. 5d that shows the mass fraction contours on different cross sections of the mixing channel. One can distinguish the double vortex formed at the T-junction (beginning of the mixing channel) that allows the partial swapping of fluids from their inlet side to the opposite side in the mixing channel. Thinner fluid lamellae, shorter diffusion lengths and, consequently, an increase of mixing are obtained when the vortices rotate with significant speed. This lasts approximately half the length of the channel (1000 μm) when Re = 250, as one can notice from the mass fraction contours. These flow

characteristics differ from those with Re = 100 (see Fig. 3) in the same design. This difference can be explained by the higher velocities of fluids in the inlet channels that make Re = 250 in the mixing channel. As it has been found in other studies [5], the centrifugal forces generated when the fluids bend at the T-junction promotes the formation of the two vortices and the increase of the contact surface of the fluids that results, in turn, on the increase of mixing with Re equal to 250 with respect to Re equal to 100.

<Fig. 5>

Fig. 6a shows a view from the outlet section of the streamlines and Fig. 6b and c show the components of velocity vectors on cross sections located at 0.4 mm and 1.6 mm of the mixing channel of design Orig2.0H, with Re = 250. Clearly, the figure resembles Fig. 4 that shows similar patterns with Re = 100. Due to the higher flow rate existing with Re = 250, the vortices formed have the same shape but they are stronger so that a weak central vortex is still present at a distance of 1.6 mm in the mixing channel. The streamlines show that when Re = 250 the two small vortices roll up and a wrapping of both fluids is produced, what is not observed with Re = 100 (see Fig. 4a).
The mass fraction contours on several cross sections of the mixing channel are shown in Fig. 6d. The magnitude of flow circulation in the channel leads to the formation of compounded lamellae of both fluids especially in the central zone of the channel cross section. The mixing is clearly enhanced in this zone. Also, the lamellae of fluids are mixed above and below the central vortex due to the two small vortices formed in the channel, but these flow structures are not present in two diagonally opposite corners which are occupied each by one fluid only, as can be seen in the contours of Fig. 6d.

<Fig. 6>

For Re = 500, previous studies [13] have found that at this order of Reynolds number the flow exhibits a transient behaviour in a T-shaped micromixer like the design AR0.5, occurring a quasi-periodic pulsating flow [25]. It has been reported that the transient regime starts at a Re value of about 240 [26].
The simulations made in this study have confirmed the transient behaviour of the flow when Re = 500 in the mixing channel. In fact, the steady simulation do not converge for Re = 500 due to the transient effects. Therefore, a transient simulation was made with a time step of 10E-05 s. The results are presented graphically in Fig. 7. In Fig. 7a, the mixing index has initially a zero value because the flow has not reached yet the outlet of the channel; this value goes up abruptly to decrease then gradually and stabilize at an approximated value of 0.06. The total time used for the analysis is 0.0009 seconds. The curves of maximum shear strain rate and wall shear stress are shown in Fig. 7b and c respectively. These show that the two physical variables start to stabilize at around 0.00045 seconds, which corresponds to the time when the curve of mixing index reaches its peak and then goes down. The stable values achieved by the variables depicted in Fig.7a-c indicate that the total simulation time used to evaluate the flow characteristics and mixing in design AR0.5 is long enough to give representative outcomes of the design.

<Fig. 7>

The low mixing index obtained in design AR0.5 with Re = 500 in the mixing channel is due to the arrangement of flow structures towards the end of the evaluation period, i.e., in 0.0009 seconds. The contact surface of fluids stays on the symmetric vertical plane of the mixing channel. This can be observed in Fig. 8 which shows the streamlines and velocity

vectors in the mixing channel. Fig. 8a shows that the streamlines do not switch from the side they come into the mixing channel to the opposite side and that basically two symmetric pairs of vortices are formed in the channel. In Fig. 8b, the components of the velocity vectors on a cross section located at 0.4 mm in the mixing channel reveal that actually eight vortices are present, four located towards the centre and other four at the corners of the channel cross section. With the loss of magnitude of the transversal velocity of flow, the vortices become in only four, which are arranged symmetrically when they are projected on a cross section of the mixing channel. This can be seen in Fig. 8b from the components of the velocity vectors on a cross section located at 1.6 mm in the mixing channel (to show them more clearly, the size of vectors at this section has been increased 10 times with respect to those on a cross section at 0.4 mm).

<Fig. 8>

Unlike the transient flow that occurs in design AR0.5 with Re = 500, a stable laminar flow still prevails in design 2.0H and, therefore, the numerical simulation gives a steady solution. The streamlines and velocity vectors in Fig. 9 reveal that the flow pattern does not differ much from the one observed with Re = 250 (see Fig. 6). In fact, the characteristics of the flow in design Orig2.0H at Re = 500 and Re = 250 in the mixing channel correspond to a laminar flow. Although strong vortices are formed in the mixing channel from the T-junction, these are in steady state and their kinetic energy decreases along the channel and it eventually dies out after some distance due to the action of fluid molecular viscosity. This indicates the absence of a vortex stretching mechanism and, thereby, the flow remains in the laminar regime. Generally, in turbulent flow, unsteady vortices appear on many scales and interact with each other. Therefore, a flow in turbulent regime can be characterized by chaotic and stochastic property changes, i.e. the flow can be highly irregular with rapid variation of pressure and velocity in space and time. This is not the case of flow at Re = 500 in design Orig2.0H but it is in design AR0.5.

<Fig. 9>

The high flow rate of Re = 500 promotes the formation of strong vortices at the entrance of the mixing channel. The vortices lose strength along the channel but the circulation is still positive at 1.6 mm distance. This leads to an increase of the mixing quality with respect to a flow with Re = 250, with mixing index increasing from 0.58 to 0.70 approximately. This can be clearly seen when comparing the mass fraction contours in Fig. 9d (Re = 500) with those in Fig. 6d (Re = 250).

The evaluation of the flow characteristics in designs AR0.5 and Orig2.0H for Re equal to 100, 250 and 500 in the mixing channel allows understanding the physics behind the mixing quality achieved in these devices. The comparison of their efficiency can also be made by plotting the values of some variables calculated numerically. The corresponding charts are shown in Figs. 10 and 11

<Fig. 10>

Fig. 10a shows that the mixing index for each Re value is higher in design Orig2.0H than in design AR0.5. The degree of mixing increases in both designs with increasing Re number in the mixing channel. In the case of design Orig2.0H, the increase of mixing index is almost negligible after 1 mm distance to the outlet section. The poor mixing that is achieved in design AR0.5 with Re = 100 and Re = 150 (in Fig. 10a, curve of Re = 100 lies over curve of Re = 150) can be understood from the streamlines in Fig. 3a which reveal the

formation of symmetrical vortices that do not disturb the interface of the fluids on the symmetry plane of the mixing channel.
In Fig. 10b, the pressure loss in the mixing channel increases with Re number in both designs. It is interesting to see that the pressure loss in the designs is of the same order with equal Re value. Therefore, higher mixing index is achieved in design Orig2.0H than in design AR0.5 without generating higher pressure loss. In this sense, the mixing performance is superior in the 3-D T-shaped micromixer.
One can note in Fig. 10c that the wall shear stress has its highest at the T-junction in both designs and it gets reduced along the mixing channel. As with the pressure loss, the level of wall shear stress is of the same order in both designs, for the same flow rates, i.e. same Re value, in the devices.
Fig. 11 shows the circulation on *Y-Z* planes located at different positions in the mixing channel. The circulation on a *Y-Z* plane, ϖ_x, is calculated by integrating the streamwise vorticity over the entire area of the *Y-Z* plane of the channel as follows:

$$\omega_x = \int_{A\ Y-Z\ plane} \left(\frac{\partial V_z}{\partial y} - \frac{\partial V_y}{\partial z} \right) dydz \tag{2}$$

<Fig. 11>

The circulation is higher at the entrance of the mixing channel and decreases along the channel for all Re numbers. In both designs, circulation is higher with increasing Re number. It is interesting to see that for Re = 250, circulation is higher in most of the cross section planes in design AR0.5 than in those in design Orig2.0H. This can be explained by the strong double vortex generated in design AR0.5 where the two vortices have the same rotational direction, whereas in design Orig2.0H three vortices are formed but the central vortex has a rotational direction opposite to the other two vortices. Nevertheless, this does not determine the level of mixing achieved, which is mostly due to the small lamellae and short diffusion lengths that enhance mixing quality.
It is important to recall that the values of Reynolds numbers (Re) used in the analysis are in a normal range for convective micromixers. It is well known that convective flow effects in the typical 2-D T-mixer only start appearing when Re is in the range of 120 to 150 [5, 14, 25]. Therefore, the Re values used are suitable to compare flow and mixing in the 3-D T-mixer and the 2-D T-mixer. In Fig. 12, some lower and higher values of Re have been also used to depict the curves of mixing index versus Re in these designs. The results confirm that the mixing performance of the 3-D T-mixer increases with Re and it is higher than that of the 2-D T-mixer over the whole range of Re. Also, the variation of mixing with Re in the simple T-mixer corresponds well to previous observations [25] that indicate the existence of different flow regimes with: 150 < Re < 250, a double vortex is created by the swapping of fluids from one side to the opposite side of the mixing channel, which enhances mixing (see Fig. 5); Re > 250, flow becomes unsteady with a periodic wake, which also makes mixing level be periodic; and, Re > 500, a parallel flow of the two fluids is formed, which decreases the mixing level since that residence time of fluids is shortened with increasing Re. In fact, the numerical simulations with Re equal to 500 and 700 in the 2-D T-mixer did not converge in steady state and the solutions were obtained in transient mode, with the values of mixing index in Fig. 12 corresponding to times of 0.0009 s and 0.0007 s respectively. Transient solutions were not required for the 3-D T-mixer with these Re values. Nevertheless, it is evident that, in both designs, much lower residence time of fluid streams with Re > 500 adversely affects the mixing level.

<Fig. 12>

5. Conclusions

Flow and mixing characteristics have been studied numerically in a proposed design that resembles a T-shaped micromixer with a three-dimensional structure formed at the T-junction due to the different horizontal levels of the inlet channels. The original design of the called 3-D T-mixer has inlet channels with cross section of h100 x w100 μm and a mixing channel of H200 x W100 μm, i.e., with aspect ratio, H/W, equal to 2.

A comparison between the original 3-D T-mixer and the typical 2-D T-mixer has been made in terms of flow characteristics, mixing level, pressure loss and maximum wall shear stress for different Re in the mixing channel. For this purpose, the commonly used T-mixer with mixing channel section of H100 x W200 μm, i.e., aspect ratio equal to 0.5, has been modelled. Thereby both designs have the same cross section areas of inlet and mixing channels.

The results show that the mixing index quickly reaches higher values in the 3-D T-mixer than in the 2-D T-mixer while pressure loss and shear stress are in the same level in both designs. For the range of Re of 100 to 500 in the mixing channel, the study confirms the flow characteristics that have been observed previously in the 2-D T-mixer [13] and it reveals different flow patterns in the 3-D T-mixer, in particular the formation of an engulfment flow even with Re = 100 which does not occur in the 2-D T-mixer. This is favoured by the design configuration which helps to occur the swapping of fluids from the T-junction between top and bottom halves of the mixing channel. The vortical flow generated in the device loses its convective strength with distance along the mixing channel, as it was evaluated through velocity vector plots and flow circulation calculation on cross sections. This decline of flow vorticity explains the poor increase of mixing, which is basically produced by diffusion from mid-length of the channel towards the outlet at 2 mm. Nevertheless, this also shows that it is only required a length of mixing channel of about 1 mm to achieve the mixing index level registered at the outlet at 2 mm, which implies lowering the pressure loss in the device by approximately 50%.

This comparative study has been applied on fixed design geometries. The results motivate to continue the analysis of flow and mixing in the 3-D T-mixer. A parametric study is to be presented where the aspect ratio of the mixing channel is discretely changed by varying the height H and the width W of the mixing channel independently and the operating conditions are set for different values of Re. Further work will be required to properly optimize [27, 28] the design geometry as well as to investigate the effects on mixing of scaling up the original device, envisaging that larger microchannels may accept higher flow rates with lower pressure loss and shear stresses.

With its simple design configuration, the 3-D T-mixer has the potential for enhancing mixing level while increasing efficiency in microsystems that include a T-junction where counterflowing fluids are put in contact to be mixed and/or to produce a chemical reaction. This can be achieved better in the 3-D T-mixer than in the typical T-mixer when the system requires high throughput with reduced losses.

References

[1] C.A. Cortes-Quiroz, A. Azarbadegan, M. Zangeneh, Characterization and optimization of a three dimensional T-type micromixer for convective mixing enhancement with reduced pressure loss, in: ASME 2010 8th International Conference on Nanochannels, Microchannels, and Minichannels Collocated with 3rd Joint US-European Fluids Engineering Summer Meeting, ICNMM 2010, 2010, pp. 1357-1364.

[2] D.M. Roberge, L. Ducry, N. Bieler, P. Cretton, B. Zimmermann, Microreactor technology: A revolution for the fine chemical and pharmaceutical industries?, Chemical Engineering & Technology, 28 (2005) 318-323.
[3] N. Kockmann, M. Engler, D. Haller, P. Woias, Fluid dynamics and transfer processes in bended microchannels, Heat Transfer Engineering, 26 (2005) 71-78.
[4] D. Gobby, P. Angeli, A. Gavriilidis, Mixing characteristics of T-type microfluidic mixers, Journal of Micromechanics and Microengineering, 11 (2001) 126-132.
[5] M. Engler, N. Kockmann, T. Kiefer, P. Woias, Numerical and experimental investigations on liquid mixing in static micromixers, Chemical Engineering Journal, 101 (2004) 315-322.
[6] S.H. Wong, M.C.L. Ward, C.W. Wharton, Micro T-mixer as a rapid mixing micromixer, Sensors and Actuators B: Chemical, 100 (2004) 359-379.
[7] H. Wang, P. Iovenitti, E. Harvey, S. Masood, Optimizing layout of obstacles for enhanced mixing in microchannels, Smart Materials and Structures, 11 (2002) 662-667.
[8] C.A. Cortes-Quiroz, A. Azarbadegan, E. Moeendarbary, An efficient passive planar micromixer with fin-shaped baffles in the tee channel for wide Reynolds number flow range, World Academy of Science, Engineering and Technology, 61 (2010) 170-175.
[9] P. Li, J. Cogswell, M. Faghri, Design and test of a passive planar labyrinth micromixer for rapid fluid mixing, Sensors and Actuators B: Chemical, 174 (2012) 126-132.
[10] R.H. Liu, M.A. Stremler, K.V. Sharp, M.G. Olsen, J.G. Santiago, R.J. Adrian, H. Aref, D.J. Beebe, Passive mixing in a three-dimensional serpentine microchannel, Journal of Microelectromechanical Systems, 9 (2000) 190-197.
[11] T.J. Johnson, D. Ross, L.E. Locascio, Rapid microfluidic mixing, Analytical Chemistry, 74 (2002) 45-51.
[12] A.D. Stroock, S.K.W. Dertinger, A. Ajdari, I. Mezi, H.A. Stone, G.M. Whitesides, Chaotic mixer for microchannels, Science, 295 (2002) 647-651.
[13] D. Bothe, C. Stemich, H.J. Warnecke, Fluid mixing in a T-shaped micro-mixer, Chemical Engineering Science, 61 (2006) 2950-2958.
[14] N. Kockmann, T. Kiefer, M. Engler, P. Woias, Convective mixing and chemical reactions in microchannels with high flow rates, Sensors and Actuators B: Chemical, 117 (2006) 495-508.
[15] N. Kockmann, T. Kiefer, M. Engler, P. Woias, Silicon microstructures for high throughput mixing devices, Microfluidics and Nanofluidics, 2 (2006) 327-335.
[16] I.D. Yang, Y.F. Chen, F.G. Tseng, H.T. Hsu, C.C. Chieng, Surface tension driven and 3-D vortex enhanced rapid mixing microchamber, Microelectromechanical Systems, Journal of, 15 (2006) 659-670.
[17] T. Matsunaga, K. Nishino, Swirl-inducing inlet for passive micromixers, RSC Advances, 4 (2014) 824-829.
[18] M.A. Ansari, K.-Y. Kim, K. Anwar, S.M. Kim, Vortex micro T-mixer with non-aligned inputs, Chemical Engineering Journal, 181-182 (2012) 846-850.
[19] Ansys, CFX 12.0, in: User Manual, 2009.
[20] Pointwise, Gridgen 15.1 User Manual, in, 2006, pp. User Manual.
[21] Ansys, CFX 11.0 User Manual, in, 2007, pp. User Manual.
[22] S. Hardt, F. Schönfeld, Laminar mixing in different interdigital micromixers: II. Numerical simulations, AIChE journal, 49 (2003) 578-584.
[23] Z. Wu, N.-T. Nguyen, X. Huang, Nonlinear diffusive mixing in microchannels: theory and experiments, Journal of Micromechanics and Microengineering, 14 (2004) 604.
[24] P.V. Danckwerts, The definition and measurement of some characteristics of mixtures, Applied Scientific Research, 3 (1952) 279-296.
[25] S. Dreher, N. Kockmann, P. Woias, Characterization of laminar transient flow regimes and mixing in T-shaped micromixers, Heat Transfer Engineering, 30 (2009) 91-100.

[26] C. Gobert, F. Schwertfirm, M. Manhart, Lagrangian scalar tracking for laminar micromixing at high Schmidt numbers, in: ASME 2nd Joint U.S.-European Fluids Engineering Summer Meeting (FEDSM2006), Miami, Florida, USA, 2006, pp. Paper no. FEDSM2006-98035 pp. 91053-91062.
[27] C.A. Cortes-Quiroz, M. Zangeneh, A. Goto, A multi-objective analysis and optimization methodology for the design of passive micromixers based on their own topology, in: AIChE Annual Meeting, Conference Proceedings, 2008.
[28] C.A. Cortes-Quiroz, M. Zangeneh, A. Goto, On multi-objective optimization of geometry of staggered herringbone micromixer, Microfluidics and Nanofluidics, 7 (2009) 29-43.

Biographies

Cesar A. Cortes-Quiroz is Research Fellow in Microfluidics & Microengineering in the Science and Technology Research Institute of University of Hertfordshire, Hatfield, UK. He graduated as BSc in Mechanical Engineering from the Pontifical Catholic University of Peru in 1995 and became an accomplished Project Engineer with extensive experience acquired across several Engineering, Procurement, Construction and Management projects in Energy, Mining & Metals and Oil & Gas. A Professional Mechanical Engineer from 2000, his genuine interest in applied sciences and engineering led him back to Academia where he completed an MSc in Mechanical Engineering in 2004 and a PhD in Microfluidics in 2010 in the Department of Mechanical Engineering of University College London, London, UK. His research interests are multi-scale fluid mechanics, design and optimization of microfluidic devices, integration of components of lab-on-a-chip and MEMS, characterization and modelling of multiphase flows and application of multiphysic solutions in microsystems.

Alireza Azarbadegan is a Professional Mechanical Engineer working at BP and Visiting Researcher and Lecturer in Design in the Department of Mechanical Engineering, University College London, UK. He obtained his PhD at the Department of Mechanical Engineering, University College London in the area of analytical and computational modelling of micropumps. His current research interests include fluid mechanics from a computational, mathematical and experimental point of view, microfluidics, and modelling and simulation of multiphysic systems.

Mehrdad Zangeneh is Professor of Thermofluids in the Department of Mechanical Engineering, University College London, UK. He obtained his BSc in Mechanical Engineering from London University and his PhD from Cambridge University. He worked as a Research Fellow in Churchill College Cambridge before joining UCL as a lecturer. Prof. Zangeneh is involved in the development of computational design methods to improve the performance of turbomachinery such as turbines, compressors, pumps, marine propulsors and waterjets. He has developed methods based on 3D inverse design and multi-objective automatic optimization. He successfully extended the multi-objective optimization procedure onto microfluidic devices such as micromixers, micropumps and structures like micro diffuser-nozzles. His research interests are in thermofluids, turbomachinery optimization and design and optimization of microfluidic devices.

Figure captions

Fig. 1 Isometric and top view of the 3-D T-shaped micromixer.

Fig. 2 (a) Cross sectional detail of the mesh used in the 3-D T-mixer geometry model, **(b)** Mixing index results from the mesh sensitivity analysis in 3D T-mixer with Re= 250. The legend indicates number of mesh cells in thousands.

Fig. 3 (a) Streamlines viewed from the outlet end, **(b)** mass fraction contours of fluorescein in water on cross sections at the inlet and outlet sections of mixing channel of design AR0.5, Re = 100.

Fig. 4 (a) Streamlines viewed from outlet section, **(b)-(c)** velocity vectors on cross sections at 0.4 mm and 1.6 mm in the mixing channel respectively, **(d)** contours of mass fraction of fluorescein in water on cross sections along the mixing channel of design Orig2.0H, Re = 100.

Fig. 5 (a) Streamlines viewed from outlet section, **(b)-(c)** velocity vector on cross-sections at 0.4 mm and 1.6 mm in the mixing channel respectively, **(d)** contours of mass fraction of fluorescein in water on cross sections along the mixing channel of design AR0.5, Re = 250.

Fig. 6 (a) Streamlines viewed from outlet section, **(b)-(c)** velocity vectors on cross sections at 0.4 mm and 1.6 mm in the mixing channel respectively, **(d)** contours of mass fraction of fluorescein in water on cross sections along the mixing channel of design Orig2.0H, Re = 250.

Fig. 7 Measurements in design AR0.5 with Re = 500 in the mixing channel: **(a)** Mixing index vs. time at the outlet section (2 mm length of mixing channel), **(b)** Maximum Shear Strain rate vs. time, **(c)** Maximum Wall Shear Stress vs. time. In (b) and (c) the evaluation is made in the whole design volume.

Fig. 8 (a) Top view (up) and view from the outlet section (bottom) of streamlines, **(b)** Tangent vectors to cross sections at 400 μm (up) and 1600 μm (bottom), in the mixing channel of design AR0.5 with Re = 500, time = 0.0009 s.

Fig. 9 (a) Streamlines viewed from outlet section, **(b)-(c)** velocity vectors on a cross section at 0.4 mm and 1.6 mm in the mixing channel respectively, **(d)** contours of mass fraction of fluorescein in water on cross sections along the mixing channel of design Orig2.0H, Re = 500.

Fig. 10 (a) Mixing index, **(b)** pressure loss, and **(c)** maximum wall shear stress (on cross section planes) in the mixing channel of designs AR0.5 and Orig2.0H for different Re numbers.

Fig. 11 Circulation on Y-Z planes (cross sections) along the mixing channel of designs AR0.5 and Orig2.0H for different Re numbers.

Fig. 12 Mixing index versus Reynolds number in the mixing channel of the 3-D T-mixer (AR = 2.0) and the simple T-mixer (AR = 0.5).

Figures

Fig. 1

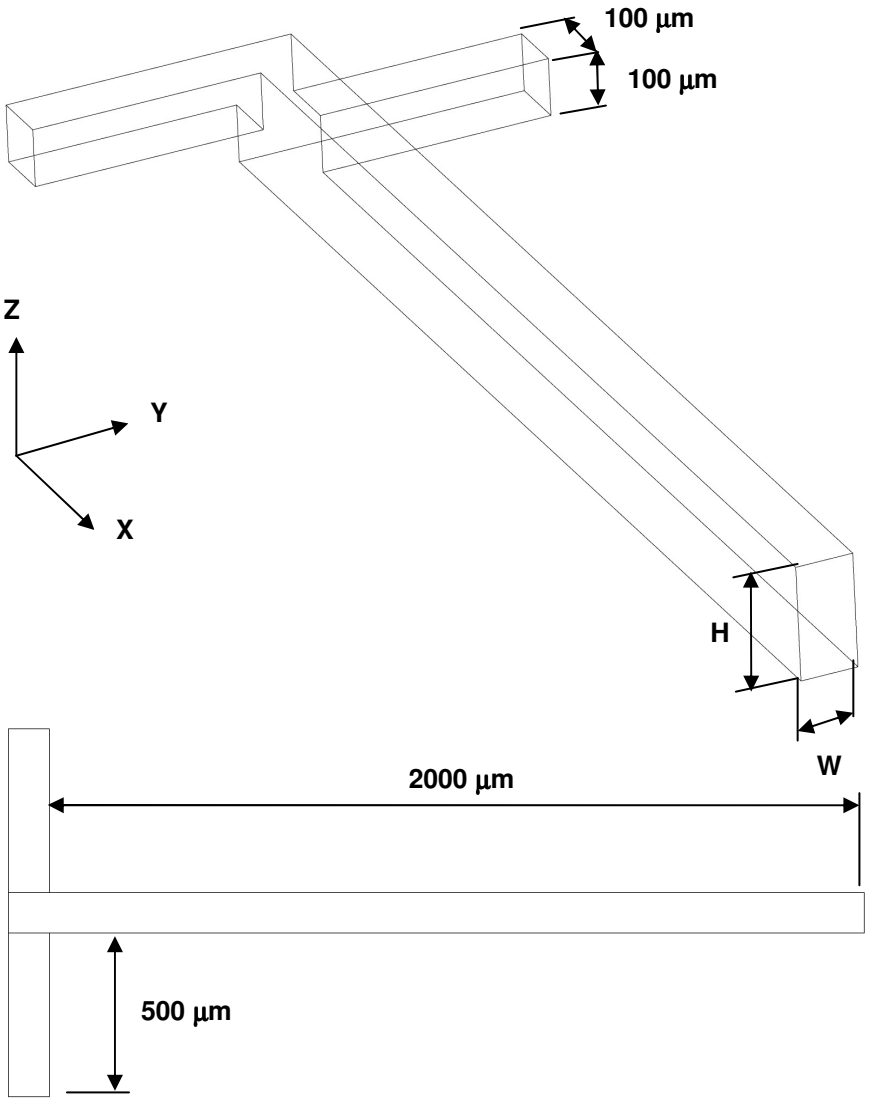

Fig. 2

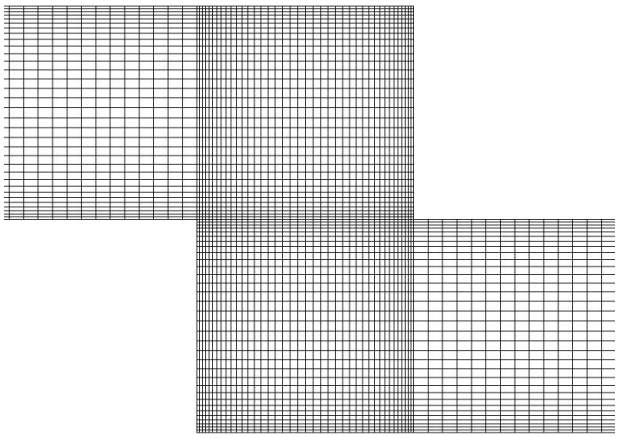

(a)

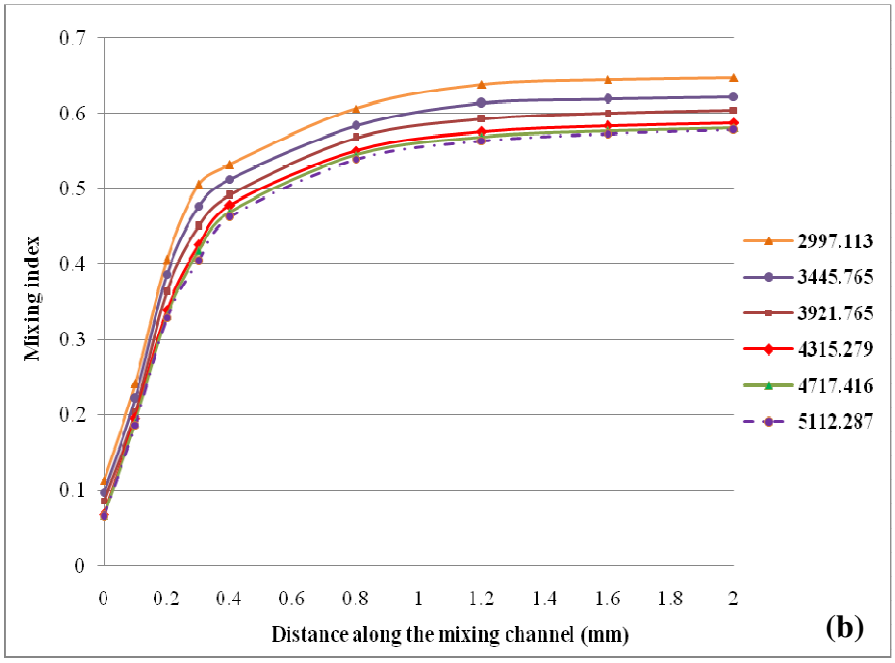
0.7
0.6
0.5
0.4
0.3
0.2
0.1
0
Mixing index
0
0.2
0.4
0.6
0.8
1
1.2
1.4
1.6
1.8
2
Distance along the mixing channel (mm)
2997.113
3445.765
3921.765
4315.279
4717.416
5112.287

(b)

Fig. 3

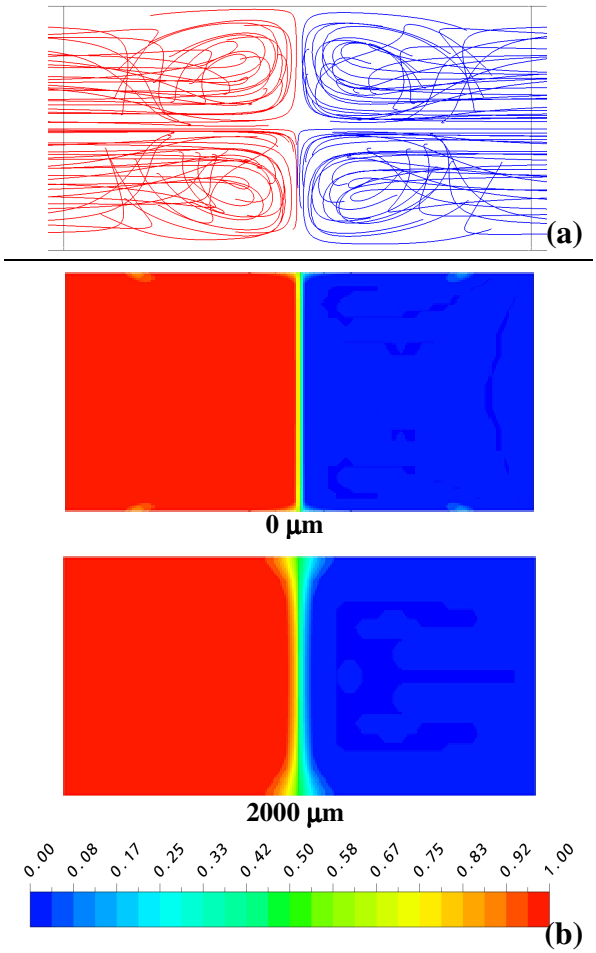
(a)
0 µm
2000 µm
0.00
0.08
0.17
0.25
0.33
0.42
0.50
0.58
0.67
0.75
0.83
0.92
1.00
(b)

Fig. 4

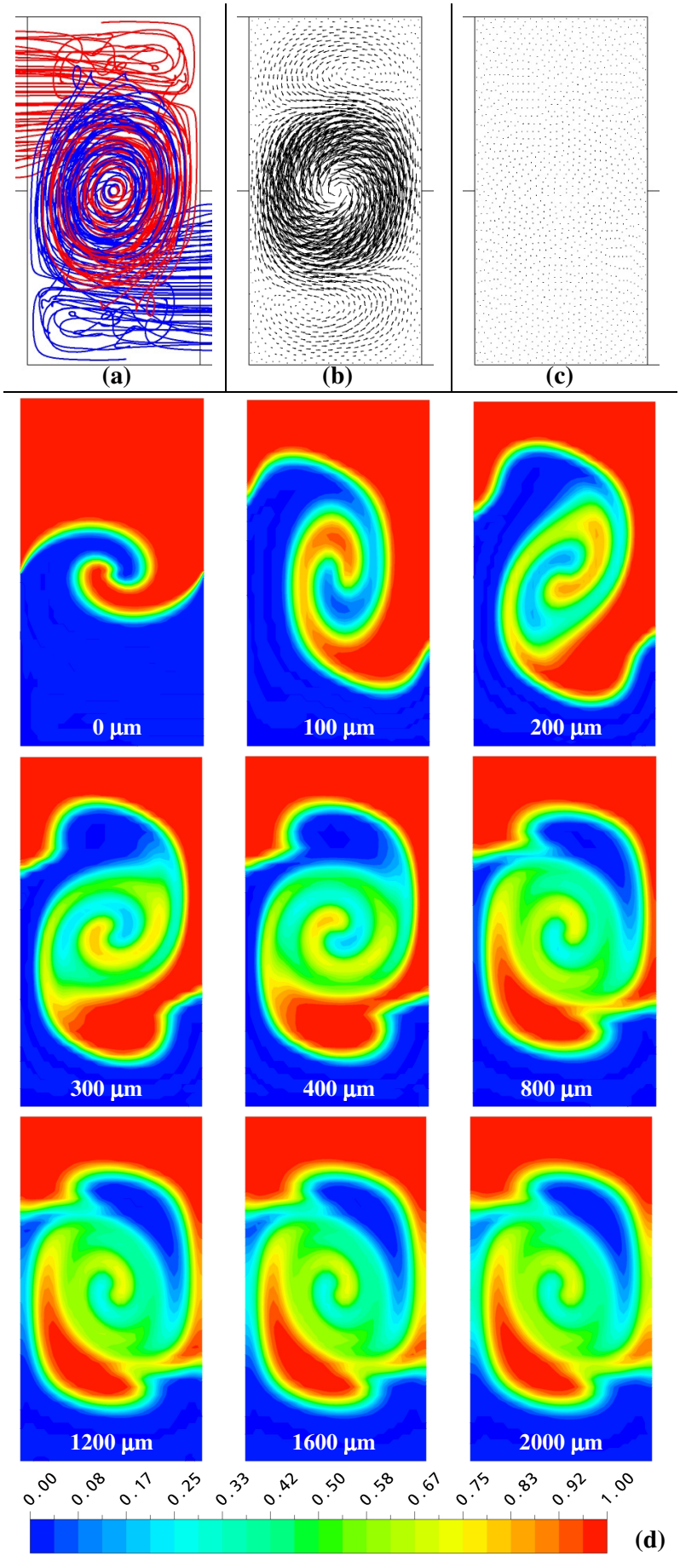
(a)
(b)
(c)
0 µm
100 µm
200 µm
300 µm
400 µm
800 µm
1200 µm
1600 µm
2000 µm
0.00
0.08
0.17
0.25
0.33
0.42
0.50
0.58
0.67
0.75
0.83
0.92
1.00
(d)

Fig. 5

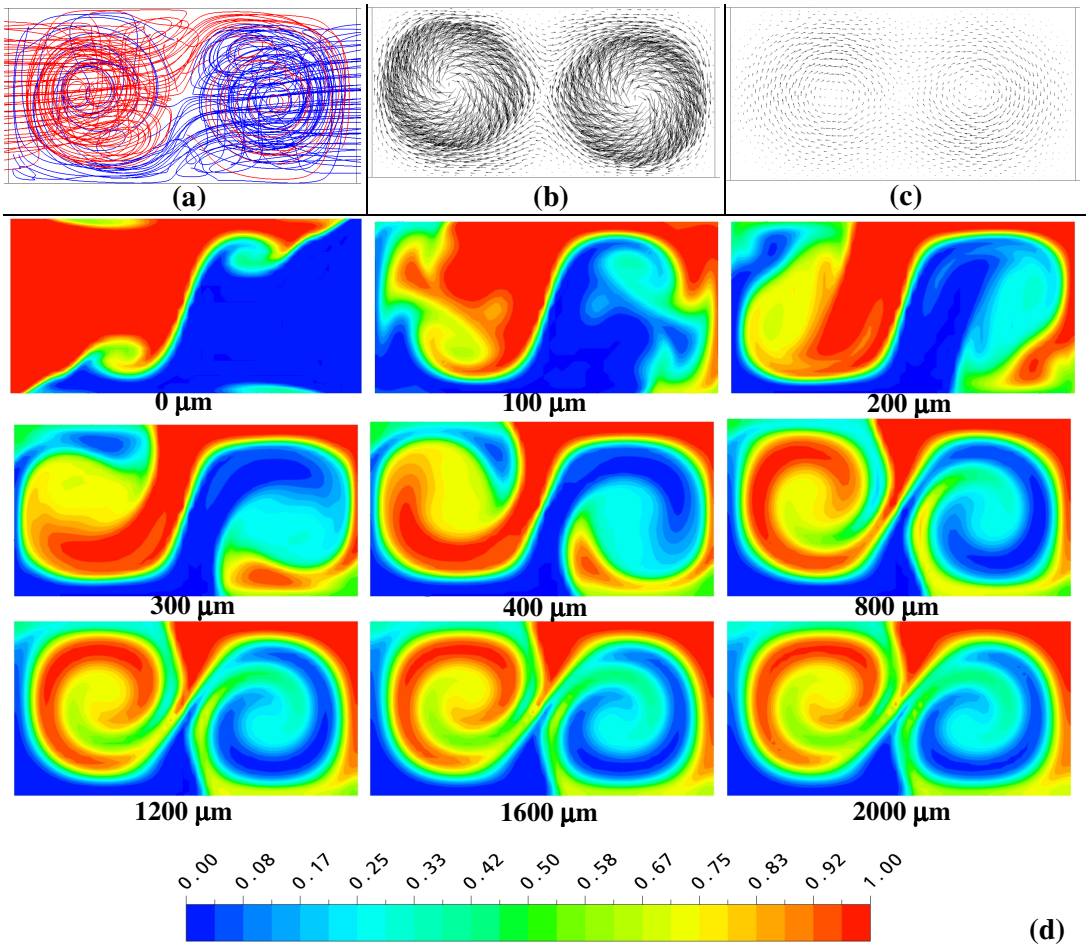
(a)
(b)
(c)
0 µm
100 µm
200 µm
300 µm
400 µm
800 µm
1200 µm
1600 µm
2000 µm
0.00
0.08
0.17
0.25
0.33
0.42
0.50
0.58
0.67
0.75
0.83
0.92
1.00
(d)

Fig. 6

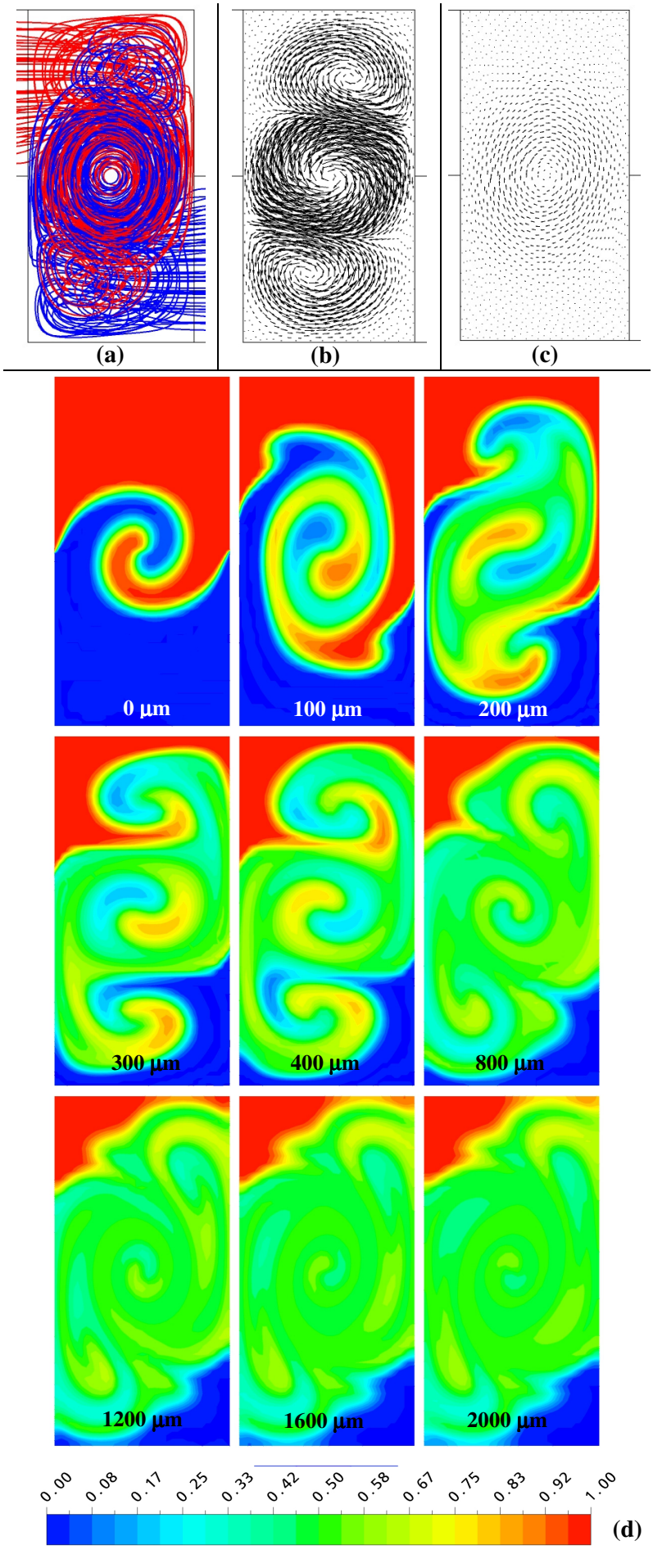
(a)
(b)
(c)
0 µm
100 µm
200 µm
300 µm
400 µm
800 µm
1200 µm
1600 µm
2000 µm
0.00
0.08
0.17
0.25
0.33
0.42
0.50
0.58
0.67
0.75
0.83
0.92
1.00
(d)

Fig. 7

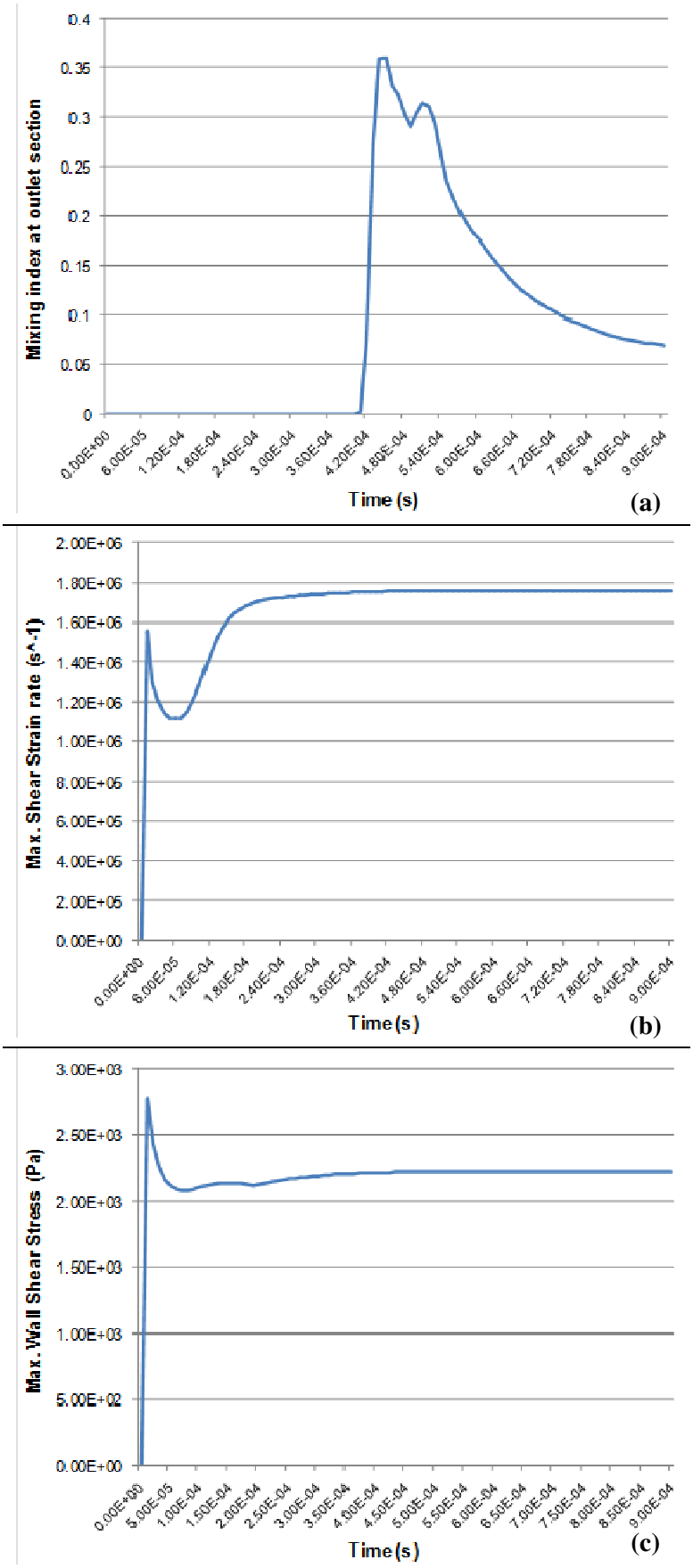
Mixing index at outlet section
0.4
0.35
0.3
0.25
0.2
0.15
0.1
0.05
0
0.00E+00
6.00E-05
1.20E-04
1.80E-04
2.40E-04
3.00E-04
3.60E-04
4.20E-04
4.80E-04
5.40E-04
6.00E-04
6.60E-04
7.20E-04
7.80E-04
8.40E-04
9.00E-04
Time (s)
(a)
Max. Shear Strain rate (s^-1)
2.00E+06
1.80E+06
1.60E+06
1.40E+06
1.20E+06
1.00E+06
8.00E+05
6.00E+05
4.00E+05
2.00E+05
0.00E+00
Time (s)
(b)
Max. Wall Shear Stress (Pa)
3.00E+03
2.50E+03
2.00E+03
1.50E+03
1.00E+03
5.00E+02
0.00E+00
Time (s)
(c)

Fig. 8

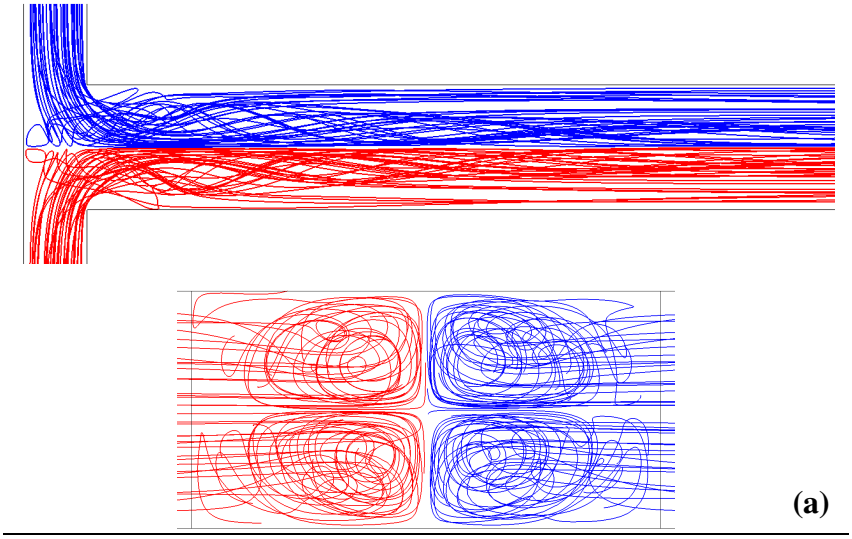

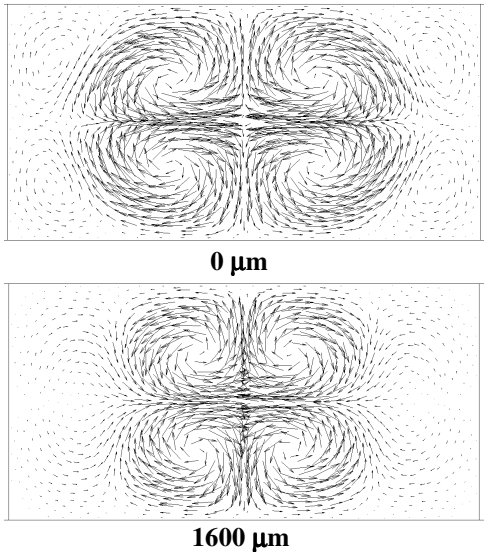

Fig. 9

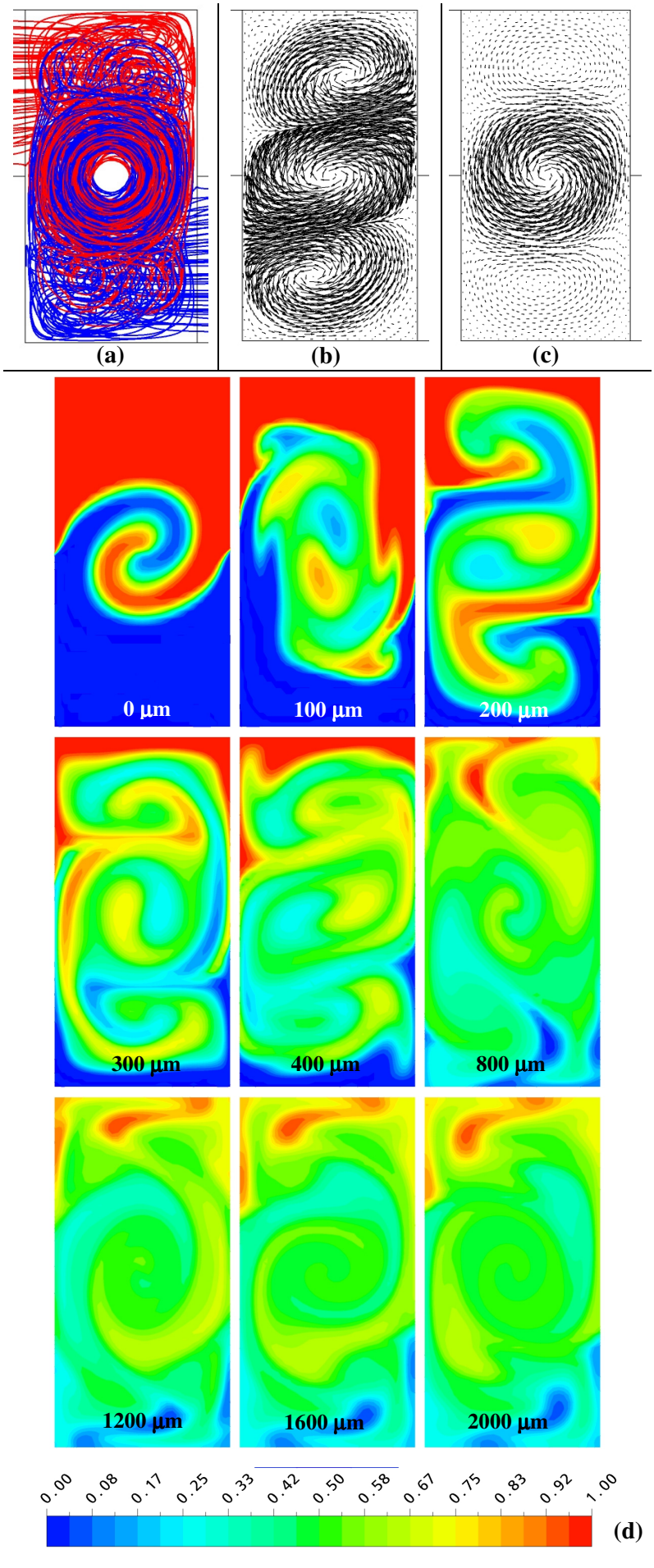
(a)
(b)
(c)
0 µm
100 µm
200 µm
300 µm
400 µm
800 µm
1200 µm
1600 µm
2000 µm
0.00
0.08
0.17
0.25
0.33
0.42
0.50
0.58
0.67
0.75
0.83
0.92
1.00
(d)

Fig. 10

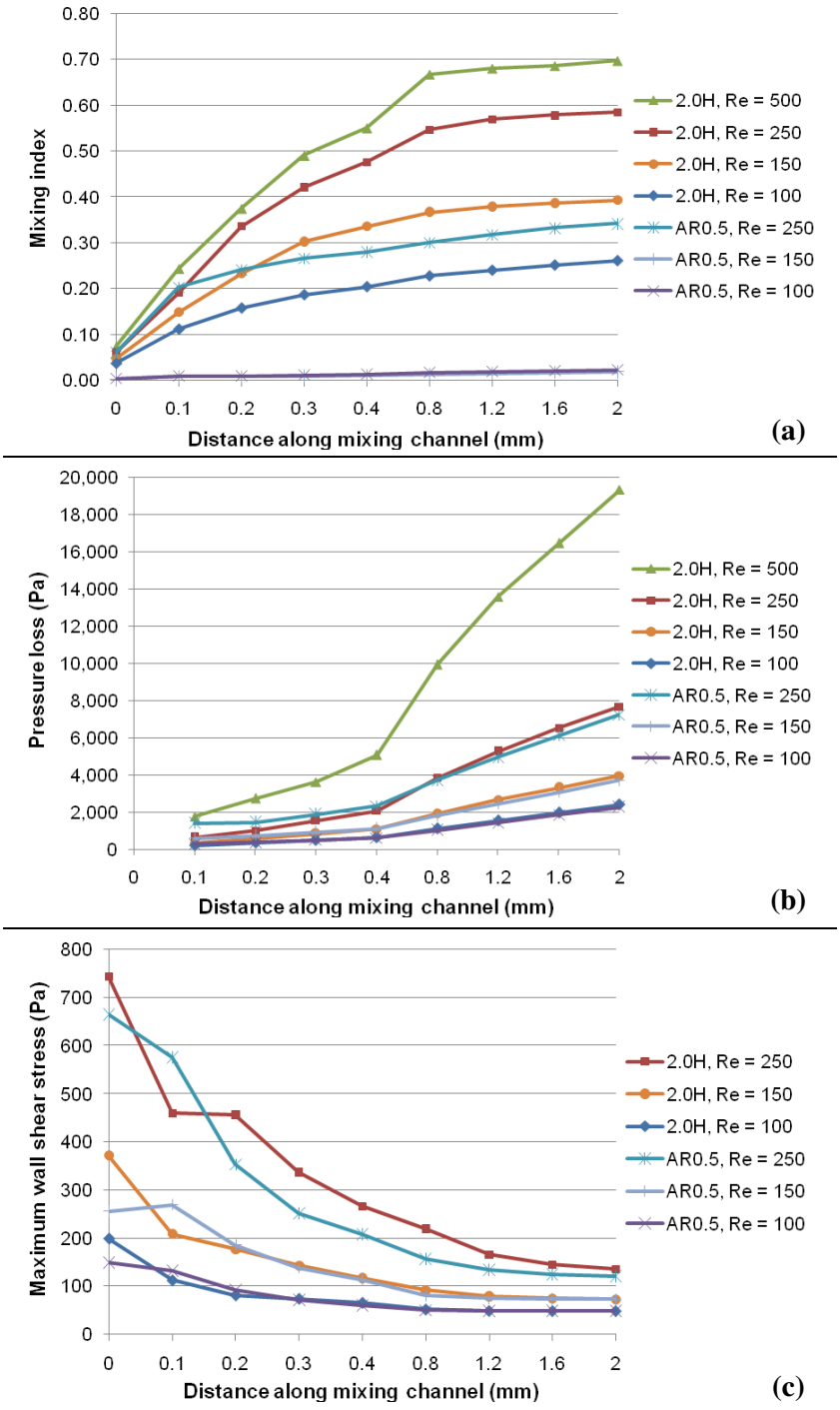
Mixing index
0.80
0.70
0.60
0.50
0.40
0.30
0.20
0.10
0.00
0
0.1
0.2
0.3
0.4
0.8
1.2
1.6
2
Distance along mixing channel (mm)
2.0H, Re = 500
2.0H, Re = 250
2.0H, Re = 150
2.0H, Re = 100
AR0.5, Re = 250
AR0.5, Re = 150
AR0.5, Re = 100
(a)
Pressure loss (Pa)
20,000
18,000
16,000
14,000
12,000
10,000
8,000
6,000
4,000
2,000
0
Distance along mixing channel (mm)
(b)
Maximum wall shear stress (Pa)
800
700
600
500
400
300
200
100
0
Distance along mixing channel (mm)
(c)

Fig. 11

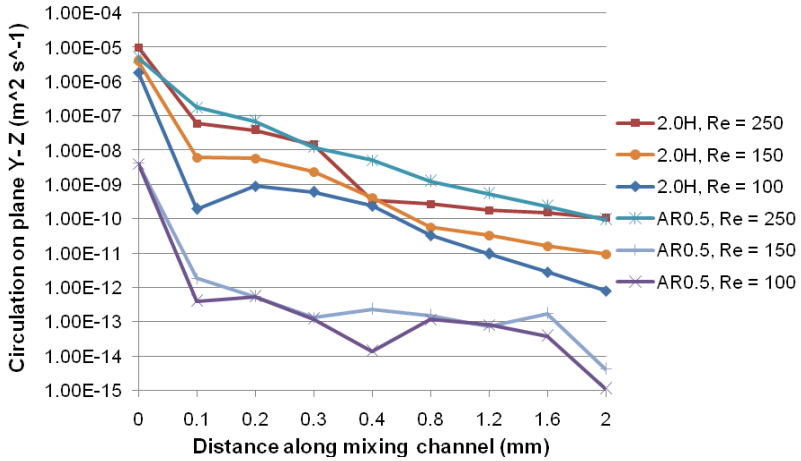
1.00E-04
1.00E-05
1.00E-06
1.00E-07
1.00E-08
1.00E-09
1.00E-10
1.00E-11
1.00E-12
1.00E-13
1.00E-14
1.00E-15
Circulation on plane Y-Z (m^2 s^-1)
0
0.1
0.2
0.3
0.4
0.8
1.2
1.6
2
Distance along mixing channel (mm)
2.0H, Re = 250
2.0H, Re = 150
2.0H, Re = 100
AR0.5, Re = 250
AR0.5, Re = 150
AR0.5, Re = 100

Fig. 12

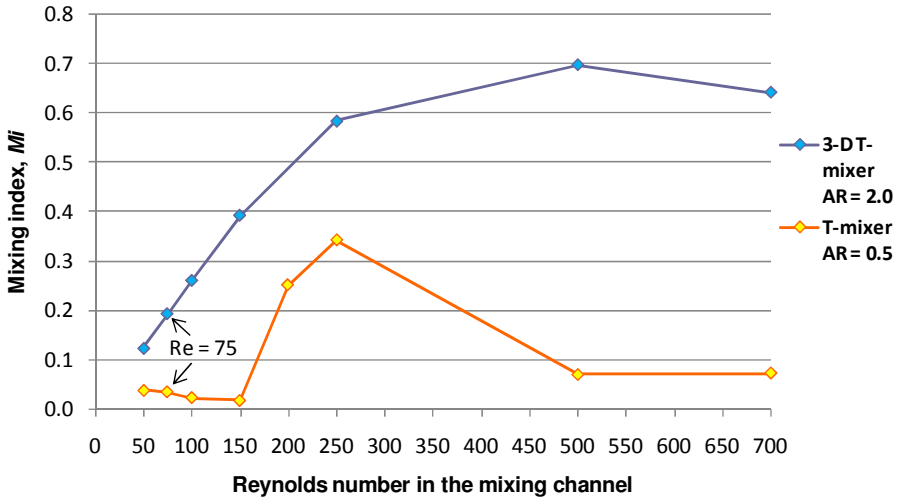
0.8
0.7
0.6
0.5
0.4
0.3
0.2
0.1
0.0
Mixing index, Mi
0
50
100
150
200
250
300
350
400
450
500
550
600
650
700
Reynolds number in the mixing channel
Re = 75
3-DT-mixer AR= 2.0
T-mixer AR= 0.5